CHAPTER III

MULTICRITICAL POINTS IN SINGLE COMPONENT LIQUID CRYSTALLINE SYSTEMS

3.1 Introduction

There is a great deal of current interest in rnulticritical points in liquid crystals. The subject matter of this chapter centres mainly on the nematic - srnectic A - smectic C multicritical point.

The scheme of presentation is as follows: A brief description of the "Lifshitz Point" is given, followed by a discussion regarding the observation of the nematic - srnectic A - smectic C rnulticritical point (or NAC point) in binary liquid crystal mixtures. Finally, our own observations of the reentrant nematic - smectic C - srnectic A (RN-C-A) and NAC multicritical points in single component liquid crystalline systems are presented. A short summary of the present theoretical understanding of the NAC point is also given.

3.1.1 Lifshitz Point

Hornreich, Luban and Shtrikrnan[1] introduced a new rnulticritical point, which they named as the "Lifshitz Point", whose critical behaviour is strikingly different from any reported previously. In order to introduce this Lifshitz Point, Hornreich et al considered the bare free energy density expression for an isotropic system, described in terms of a scalar order parameter M,

$$F(M) = a_2 M^2 + a_4 M^4 + a_6 M^6 + \ldots + c_1 (\nabla M)^2 + c_2 (\nabla^2 M)^2 \qquad [1]$$

The point at which the coefficient c_1 changes sign and c_2 is positive is the Lifshitz Point. An example of a phase diagram exhibiting such a Lifshitz Point is given in fig.3.1. From the figure it is seen that as one moves from 1 to 2 along the λ line of second order phase transitions by varying a parameter P, the ordered state changes from ferromagnetic to helicoidal. This could be achieved, for example, by varying the pressure or composition of alloys. The wave vector k characterising the helicoidal structure increases continuously from $k = 0$ at the Lifshitz Point L.

3.1.2 NAC Multicritical Point

The NAC multicritical point was first theoretically predicted and found later experimentally. When it was initially suggested, the two proposed explanations were very different. Chu and McMillan[2] (CM) proposed a model in which smectic C had the dipolar order parameter of McMillan's theory,[3] while the smectic A order parameter was the one-dimensional density wave of Kobayashi, McMillan and de Gennes.[4] Tilt of the director away from the layer normal enters the CM model somewhat incidentally through a gradient term coupling the two order parameters. Chen and Lubensky[5] (CL) found a NAC point in a model where the only order parameter was the one-dimensional density wave. Tilt of the director relative to the layer normal is a central feature of this model and the NAC point is obtained when the coefficient of the transverse gradient term becomes negative. The model predicted a phase diagram as shown in fig.3.2.

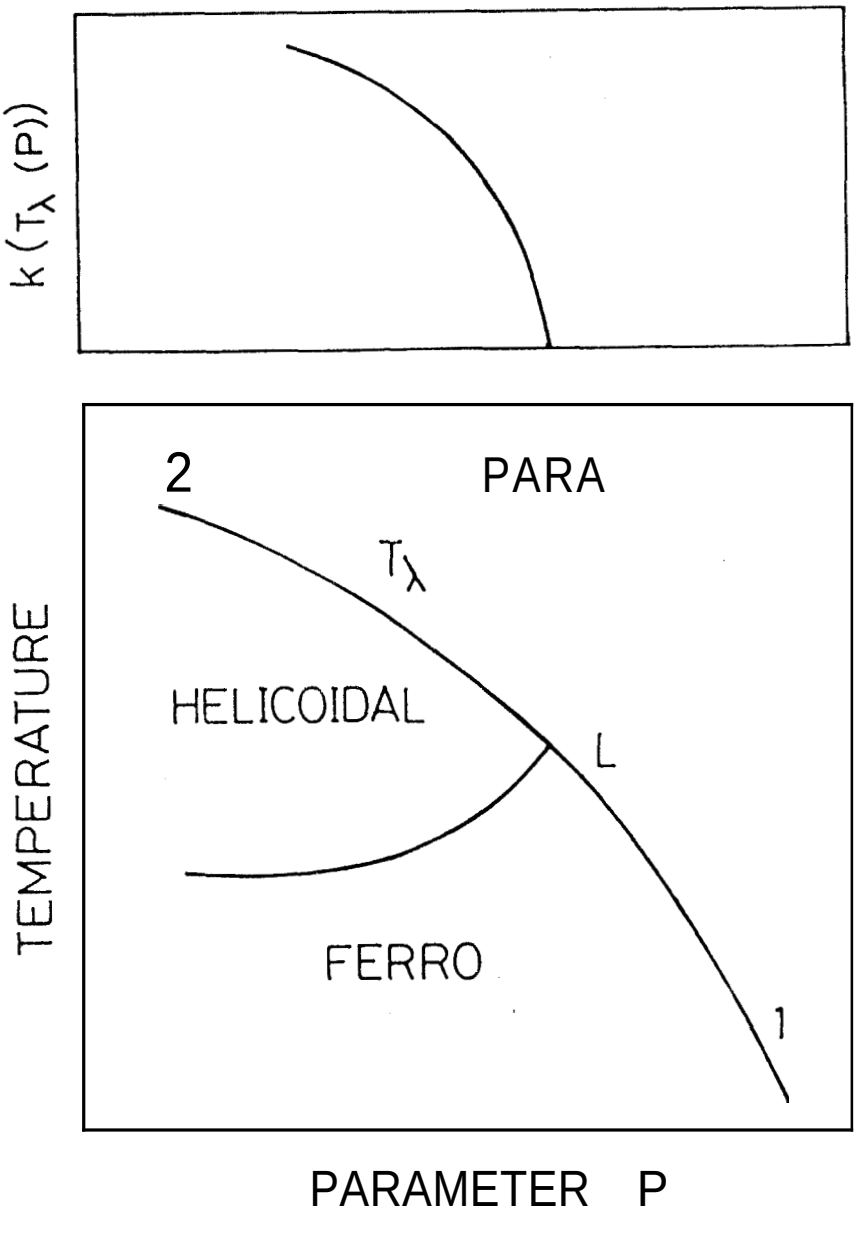

Figure 3.1 Schematic phase diagram of a magnetic system exhibiting a Lifshitz point L. The curve 1-2 is the λ line of second-order phase transitions. The upper figure shows the equilibrium wave vector k of the helicoidal and ferromagnetic phases on the λ line (from ref.1)

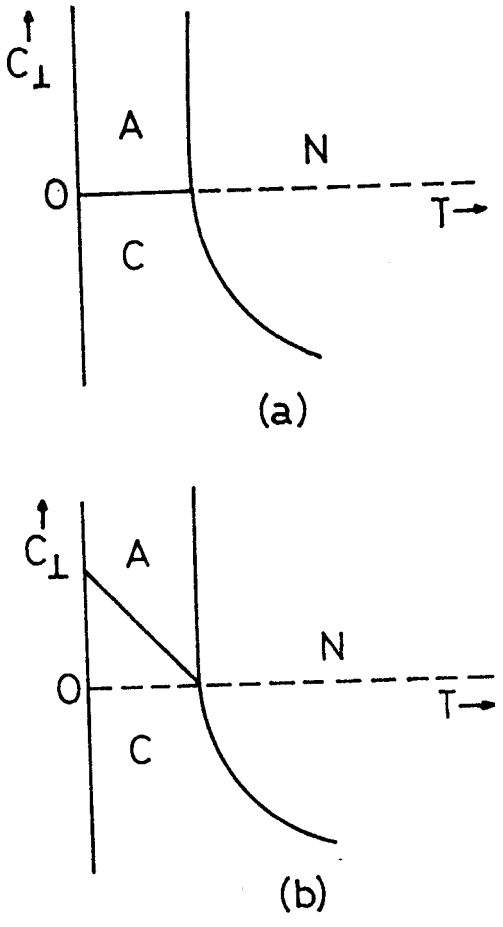

Figure 3.2 Phase diagram of the system showing NAC point predicted by the CL model (a) before (b) after refinement (from ref. 5)

Differences between the two models are quite substantial. In the CL model, for example, the NAC point is a type (m = 2) of Lifshitz point, which leads to the prediction that the Xray scattering in the nematic phase near the NAC point falls off in the transverse direction as $q_{\perp}^{-4}$, rather than the usual $q_{\perp}^{-2}$ behaviour predicted by the CM model. Furthermore, the nematic-smectic C (NC) transition entropy is zero in the CM model, but is expected to be finite in the CL model owing to fluctuations.[1,6-8]

The first experimental observation of the NAC point was by Johnson et al.[9] Using differential scanning calorimetry and thermal microscopy, they reported that the temperature-concentration (T-X) diagram of octyloxy-and heptyloxy-p-pentyl phenyl thiol benzoate ($\bar{8}S5$ and $\bar{7}S5$) exhibits a NAC point (fig. 3.3). One of these compounds, namely, $\bar{8}S5$ shows nematic, srnectic A and smectic C phases, while the other ($\bar{7}S5$) shows only nematic and srnectic C phases. Addition of $\bar{7}S5$ to $\bar{8}S5$ decreases the smectic A range and finally for concentrations above 42% of $\bar{7}S5$ (mole %), the nematic phase directly goes to the smectic C phase resulting in a NAC point. Differential scanning calorimetry experiments led to the following observations:

a) A-C transitions are continuous and do not show any pretransitional effects.

b) A-N transitions are continuous and show strong pretransitional effects which vanish as the NAC point is approached (see fig.3.4b).

c) N-C transitions are weakly first order and show very weak pretransitional effects (see fig.3.4a). The NC transition entropy vanishes

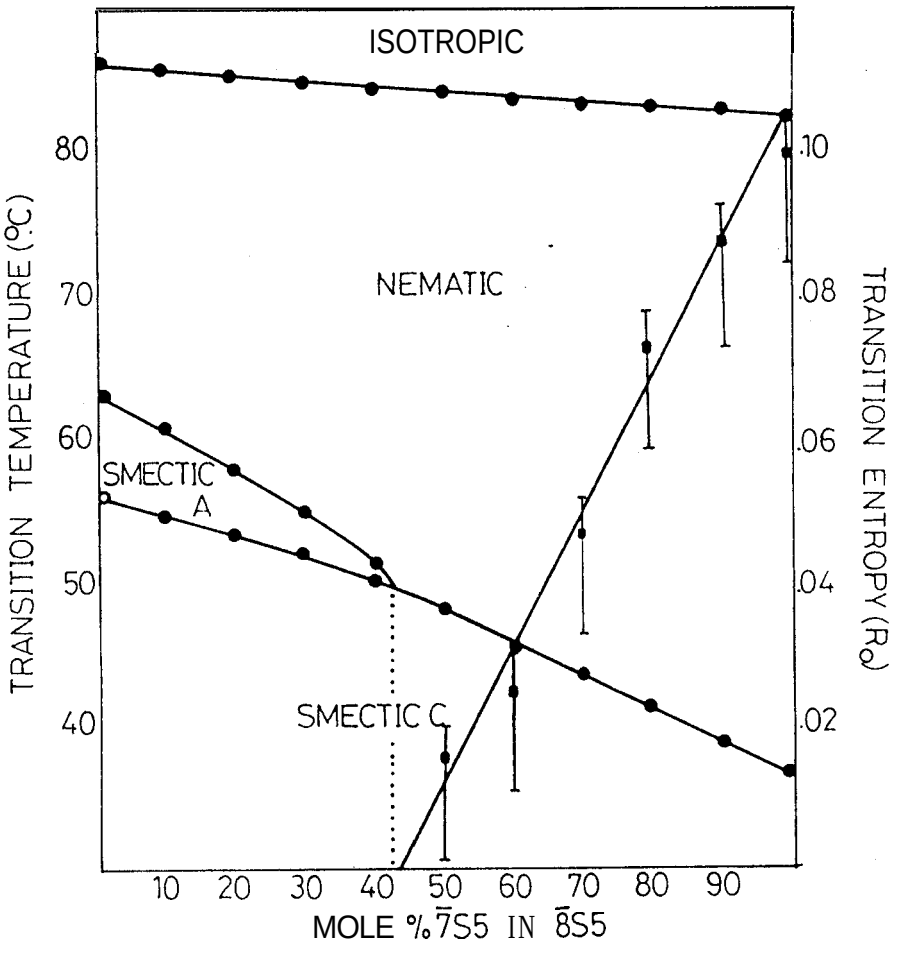

Figure 3.3 Isobaric temperature-concentration phase diagram of 8S5 and 7S5. Solid circles represent phase transition temperatures. The solid squares represent the NC transition entropy (from ref. 9)

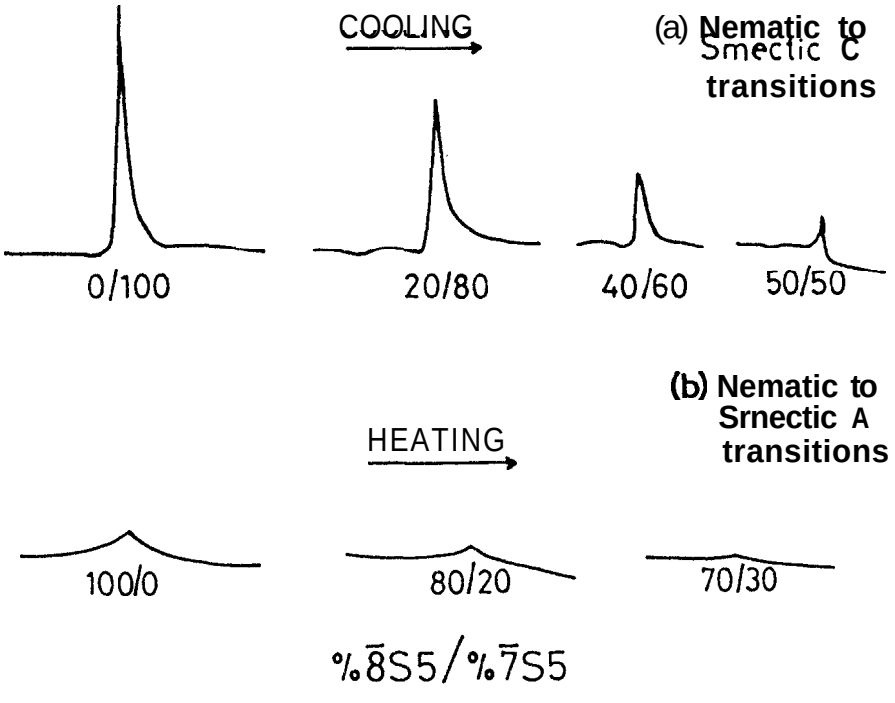

Figure 3.4 a) DSC traces of the nematic-smectic C transitions of several 8S5/7S5 mixtures illustrating the rapid decrease of transition entropy as the multicritical point is approached.

b) DSC traces of the nematic-smectic A transitions of several mixtures of 8S5 and 7S5. The traces show the weakening of the transitions as the multicritical point is approached.

Numbers below the traces indicate the respective concentrations of 8S5 and 7S5 in the mixture (from ref. 9)

as the NAC point is approached.

d) The point where the three phase transition boundaries (NA, NC and AC) meet is a multicritical point. At that point the three phases become indistinguishable.

Johnson et al[9] also formulated a phenomenological Landau theory to give a qualitative description of the observed phase diagram. Sigaud and co-workers[10] independently reported another system which showed a NAC point, again in the T-X plane. The compounds used were 4'-octyloxy-4-cyano biphenyl (8OCB) and 2p-n-heptyloxy amino fluorenone (7ONE). The topology of the phase diagram (fig.3.5) is apparently different from that of Johnson et al.[9] These experiments were followed by accurate high resolution calorimetric[11,12] and Xray experiments,[13] which permitted explicit comparisons with the theoretical predictions.

Recently, Brisbin et al[14] have obtained high resolution phase diagrams of four binary liquid crystal systems exhibiting the NAC point. Fig. 3.6 displays these phase diagrams in the vicinity of the NAC points. It is seen that these phase diagrams have substantial quantitative differences between them. Brisbin et al[14] argued that the reason for this can be threefold.

i) Materials, such as 8OCB, neither exhibit the smectic C phase nor would they even if supercooled to very low temperatures; thus a slight increase in 80CB concentration strongly suppresses the C phase and hence the A-C boundary. This is unlikely in the case of $\bar{8}$S5 and 9S5

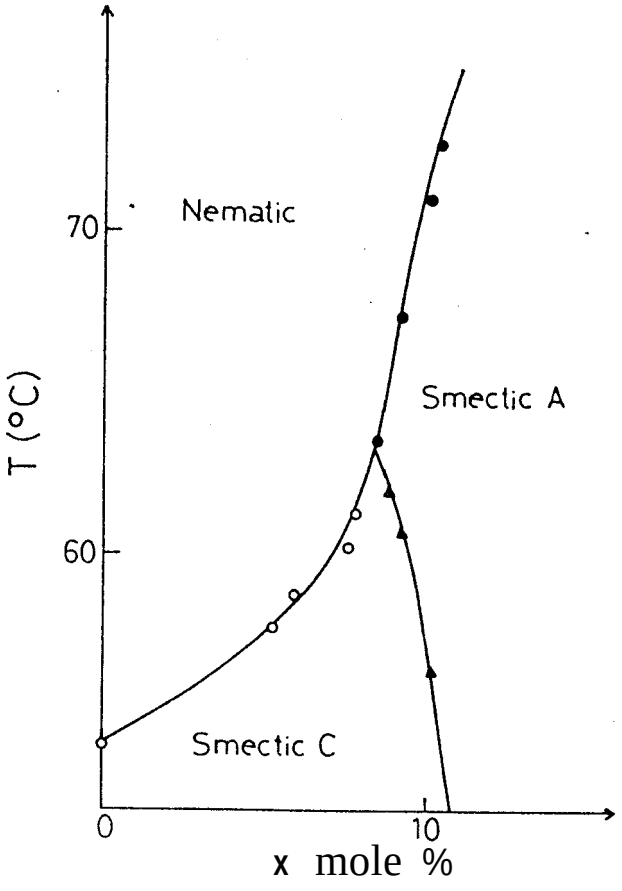

Figure 3.5 Isobaric temperature-concentration phase diagram of 7ONE-8OCB system (from ref. 10)

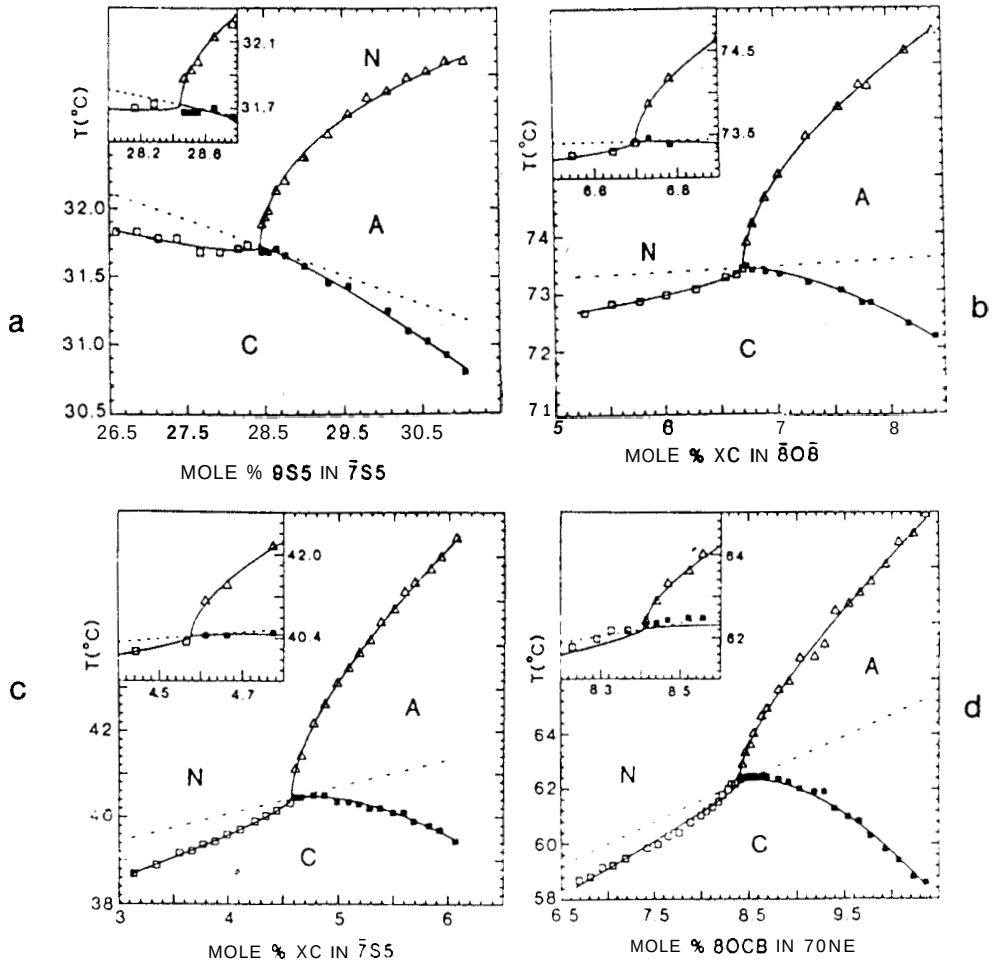

Figure 3.6 High resolution temperature concentration phase diagrams of

a) 4-n-pentyl-phenyl thiol-4'-nonylbenzoate (9S5) and 4-n-pentyl-phenyl thiol-4'-heptyloxybenzoate (7̄S5)

b) 4-propionylphenyl-trans (4-n-pentyl)cyclohexane carboxylate (XC) and 4-n-octyloxyphenyl-4'-n-octyloxybenzoate (8O8̄)

c) 4-propionylphenyl-trans(4-n-pentyl)cyclohexane carboxylate (XC) and 4-n-pentyl-pentyl thiol-4'-heptyloxybenzoate (7̄S5)

d) 4'-octyloxy-4-cyanobiphenyl (8OCB) and 2p-n-heptyloxy-benzylidene amino fluorenone (7ONE)

The insets show the diagram close to the NAC point (from ref. 14)

as they either have smectic C phase or would have it if slightly supercooled; thus the A-C line is unsuppressed or only mildly suppressed.

ii) The amplitude of the leading singularities of the AN and NC lines vary by a factor of about 4.

iii) The non singular background slope on which the singularity is superimposed varies considerably and even changes sign (see dashed line in fig. 3.6).

The authors provided quantitative evidence to show that inspite of gross differences in global features, universality rules near the NAC point. This was done in the form of relationships between the parameters describing the AN and NC boundaries, viz., the exponent η and the amplitudes A_{NA} and A_{NC}, the parameters being defined by the following expressions.

$$T_{NA} - T_{NAC} = A_{NA} (X_{NA} - X_{NAC})^{\eta} + B(X_{NA} - X_{NAC}) \qquad [2a]$$

$$T_{NC} - T_{NAC} = A_{NC} (X_{NAC} - X_{NC})^{\eta} + B(X_{NAC} - X_{NC}) \qquad [2b]$$

Here X is the mole fraction of the constituent having the smectic A phase.

The results of fitting the data of Brisbin et al to equations [2a] and [2b] with and without the universality constraints on η and the amplitude ratio A_{NA}/A_{NC} are given in Table 3.1. Solid lines in fig. 3.6 show that fits constrained to have universal values are excellent except for 7ONE/8OCB data which exhibit small systematic deviations, probably because of experimental artefacts as discussed above. Goodness of fit is objectively indicated by the small in-

TABLE 3.1

Best-fit parameters and values of χ^2 for fits of data by equations of the form of Eqs. (2). See the text for details and discussion. Numbers in parentheses exclude 7ONE/8OCB. $R = A_{NA}/A_{NC}$. (From ref. 14)

	$\bar{7}S5/9S5$	$\bar{8}0\bar{8}/XC$	$\bar{7}S5/XC$	7ONE/8OCB
η	0.77±0.14	0.56±0.03	0.55±0.02	0.78±0.08
R	-1.9±1.0	-5.8±2.0	-9.8±4.0	-1.7±0.4
A_{NC}	-30±48	-6.7±3.5	-5.0±2.6	-161±147
B	-78±77	8.4±16	83±16	-160±230
		χ^2 = 1.015 (0.924)		
η		0.573±0.02 (0.556±0.02)		
R		-5.96±1.3 (7.63±2.2)		
A_{NC}	-2.6±0.9 (-1.9±0.7)	-6.9±2.3 (-4.9±2)	-9.4±3.1 (-6.6±2.6)	-10.3±3.4
B	-20±4.2 (-18±4)	8±10 (18±10)	63±13.6 (75±13)	157±16
		χ^2= 1.162 (1.00)		
η_{AC}	1.76±0.3 (1.71±0.3)	1.4±0.07 (1.41±0.1)	1.47±0.04 (1.48±0.04)	1.6±0.04
		χ^2 = 0.869 (0.914)		
η_{AC}		1.52±0.03 (1.46±0.03)		
		χ^2 = 0.977 (0.919)		

crease of X^2 that accompany the application of universality constranits. Dashed lines in the figures represent the best fit slope (B) term in equations [2a] and [2b] with the constraints in effect. Solid lines through the AC data represent equations of the form [2a] and [2b] wherein the values of B, X_{NAC} and T_{NAC} obtained from the NA/NC fits have been used, along with the constraint that η_{AC} is universal for all the four systems. Again the fits are very good. Thus Brisbin et al showed that with a simple choice of the scaling axes, the NAC diagrams exhibit quantitative universality.

Since all these studies have been on binary systems, the need arises to observe the NAC point in a single component liquid crystal system in the pressure-temperature (P-T) plane to test the concept of universality near such a point, since it is unlikely that both density and concentration fluctuations would produce the same topological distortion of the phase diagrams. With a view to find such a point, in the P-T plane, Shashidhar et al[15,16] undertook experiments on several systems. Of particular mention are those on n-(4-n-pentyloxy benzylidene)-4'-n-hexylaniline (50.6), $\bar{8}S5$, $\bar{7}S5$ and their mixtures. The P-T diagram obtained for 50.6 is given in figs. 3.7 and 3.8. Though the range of the smgctic A phase decreased with increasing pressure, it never got bounded in the range of the pressure studied (about 8kbar). As already mentioned mixtures of $\bar{7}S5$ and $\bar{8}S5$ show nematic, smectic A and smectic C phases for $X \leq 0.42$ (where X is the mole fraction of $\bar{7}S5$ in the mixture) and only nematic and smectic C phase for $X > 0.42$, resulting thus in a NAC point in the T-X plane at $X \simeq 0.42$. So both the pure compounds and their binary

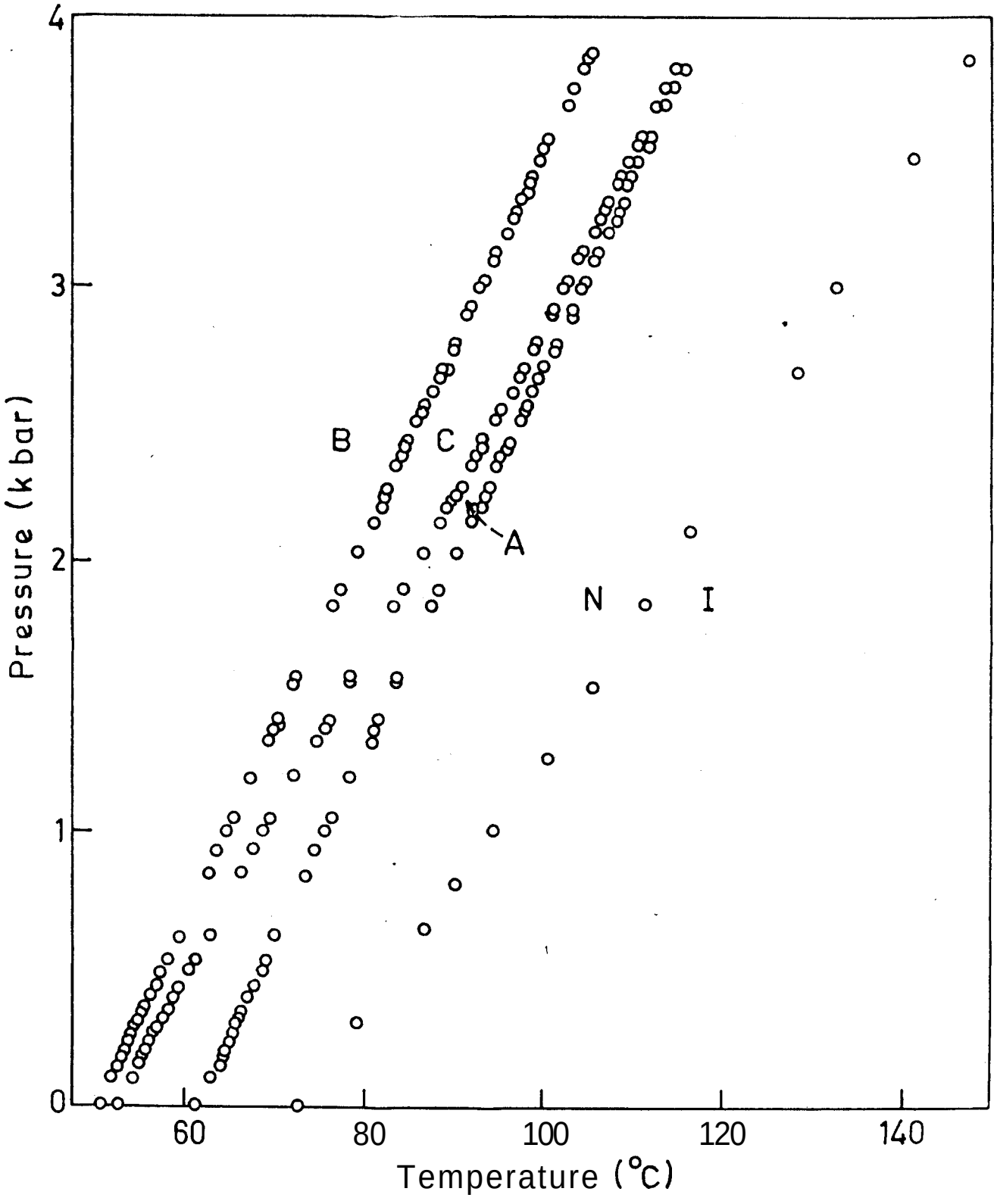

Figure 3.7 P-T diagram of 50.6 upto 4 kbar (from ref. 15)

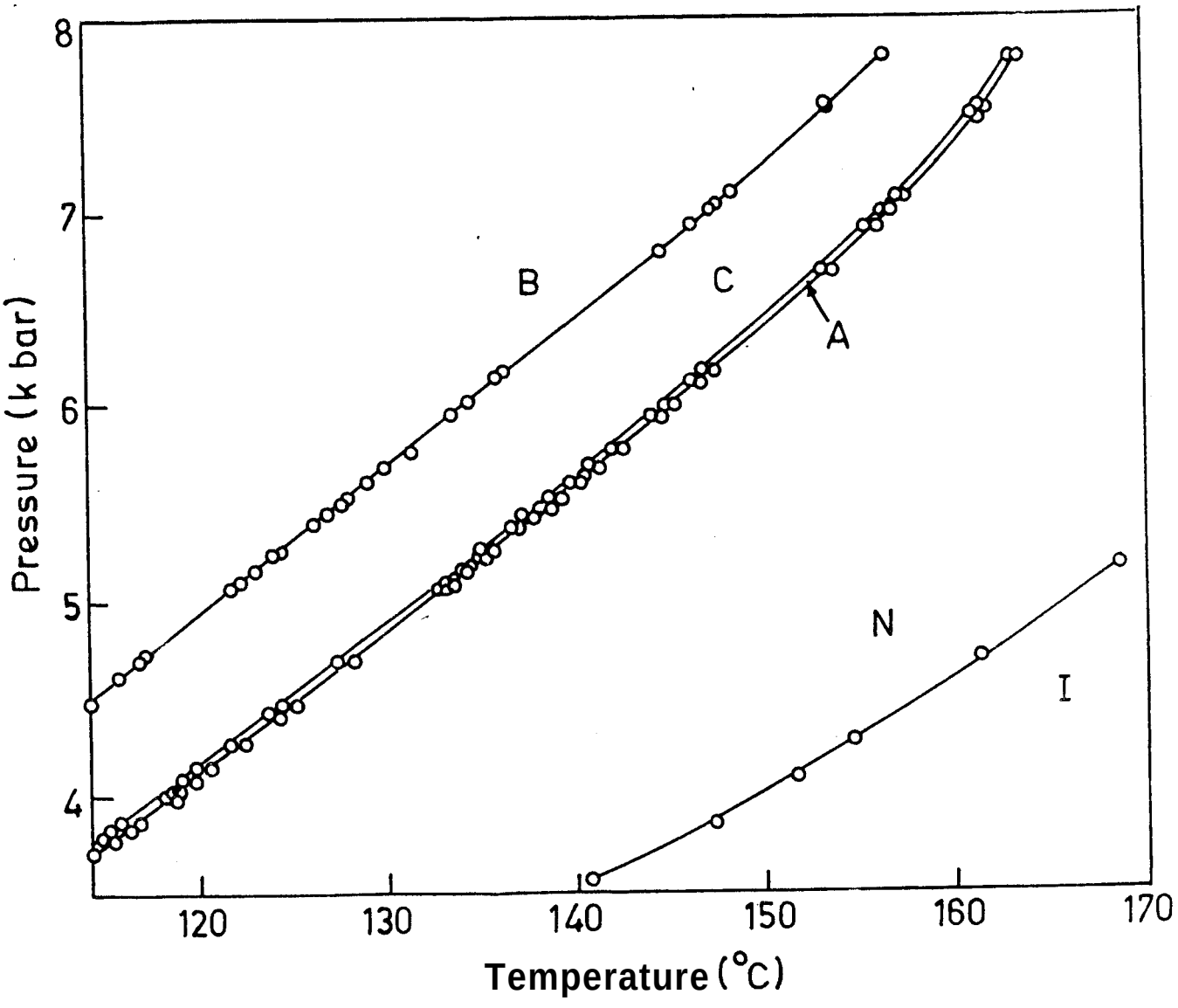

Figure 3.8 P-T diagram of 50.6 from 4 kbar to 8 kbar (from ref. 15)

mixtures whose concentration was close to X = 0.42 were considered to be potential candidates to observe a NAC point in the P-T plane. But as it turned out neither the pure compounds nor their mixtures could produce a NAC point in the P-T plane.[16]

Continuing their efforts to look for a NAC point in single component systems, Shashidhar, Kalkura and Chandrasekhar[17,19] observed a new kind of multicritical point. Pressure studies were done on 4-(4"-n-decyloxy-benzoy1oxy)-benzylidene-4'-cyanoaniline[18] (hereafter abbreviated as DOBBCA) which has the following sequence of transitions.

$$I \longrightarrow N \longrightarrow S_A \longrightarrow S_C \longrightarrow RN \longrightarrow K$$

These studies led to the first observation of a multicritical point (RN-C-A point) in a single component liquid crystalline system. The precision in these measurements did not permit definitive conclusions regarding the topology of the phase boundaries in the immediate vicinity of the RN-C-A point. In this chapter we present the precise data obtained close to the RN-C-A point. This chapter also describes the results of the high resolution pressure studies on 4-n-heptacyl phenyl-4'-(4"-cyanobenzoyloxy)benzoate (7APCBB for short) which led to the first observation of the NAC point in a single component system. From the high resolution P-T diagram of 7APCBB we shall show that the topology of the phase diagram is indeed universal near the NAC point. We shall also attempt to explain why the topology of the RN-C-A point diagram is apparently different.

3.2 Materials

a) DOBBCA: The chemical structure of this compound is shown in fig.3.9. On cooling from the isotropic phase it exhibits the nematic, smectic A, smectic C and reentrant nematic phases. Transition temperatures as determined by using a polarising microscope equipped with a programmable hot stage (Mettler FP5/FP52), are given in Table 3.2.

b) 7APCBB: Fig.3.10 shows the chemical structure of 7APCBB. The transition temperatures of this compound, which on cooling from isotropic phase shows nematic, smectic A and smectic C phases are given in Table 3.3.

3.3 Experimental:

The experiments were carried out using the high pressure optical cell described in chapter II. The phase transitions were detected by monitoring the intensity of the laser light transmitted by the sample. Experiments were always conducted along isobars i.e., the transition temperature was determined by keeping the pressure constant and varying the temperature at a uniform rate. As mentioned earlier, the accuracy with which the experiments were done on DOBBCA earlier[17] was not sufficient to map out the precise topology of the phase diagram in the proximity of the RN-C-A point. In the present experiments a pressure transducer (BLH, Waltham USA) has been used so that pressure could be monitored and measured electronically. This improved the accuracy of the pressure measurement significantly. The precision which was

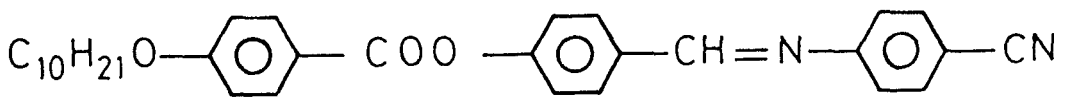

4 (4 - n - decyloxy - benzoyloxy) benzylidene - 4′ cyanoaniline

Figure 3.9 Chemical structure of DOBBCA

TABLE 3.2

Transition Temperatures (at atmospheric pressure) of DOBBCA

Transition	Short Form	Temperature (°C)
Reentrant Nematic - Smectic C	RN-C	(64.3)
Smectic C - Smectic A	C-A	73.3
Smectic A - Nematic	A-N	232.1
Nematic - Isotropic	N-I	242.0

( ) indicates that the transition is monotropic

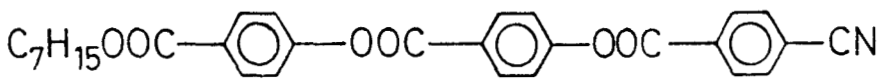

4 – n – heptacylphenyl – 4'– (4''– cyanobenzoyloxy) benzoate

Figure 3.10 Chemical structure of 7APCBB

TABLE 3.3

Transition Temperatures (at 1 bar) of 7APCBB

Transition	Short Form	Temperature (°C)
Smectic C - Smectic A	C - A	141.6
Smectic A - Nematic	A - N	144.4
Nematic - Isotropic	N - I	209.4

±15 bar in the earlier experiments is improved to ±0.3 bar. Also the precision of the temperature measurement is ±0.025 K in the present experiments compared to ±0.05 K of the earlier experiment. The rate of variation of temperature was about 1 K/min.

For the 7APCBB experiments further improvement in precision was incorporated: the rate of heating was 0.25 K/min and the accuracy of the temperature measurement was 20 mK or better. In the preliminary experiments conducted with the purpose of locating the NAC point in the P-T plane, the accuracy of the pressure measurement was ±0.7 bar. For obtaining very precise data in the vicinity of the NAC point, pressure had to be elaborately monitored during every run. In these high resolution experiments, pressure was determined to a precision of t0.1 bar and was constant to within the same limits during any run.

3.4.Results and Discussion

3.4.1 Studies on the RN-C-A Point

The complete P-T diagram of DOBBCA obtained by Shashidhar et al[17] is given in fig.3.11. It is seen that the range of the C phase which is 11.1°C at 1 bar decreases drastically with increasing pressure and finally at 0.5 kbar, the C phase is suppressed. This results in the RN-C-A point. As remarked already the precision of pressure measurements in the earlier studies[17] was not sufficient to make definitive statements concerning the topology of the P-T diagram close to the RN-C-A point. But what is unmistakable is that

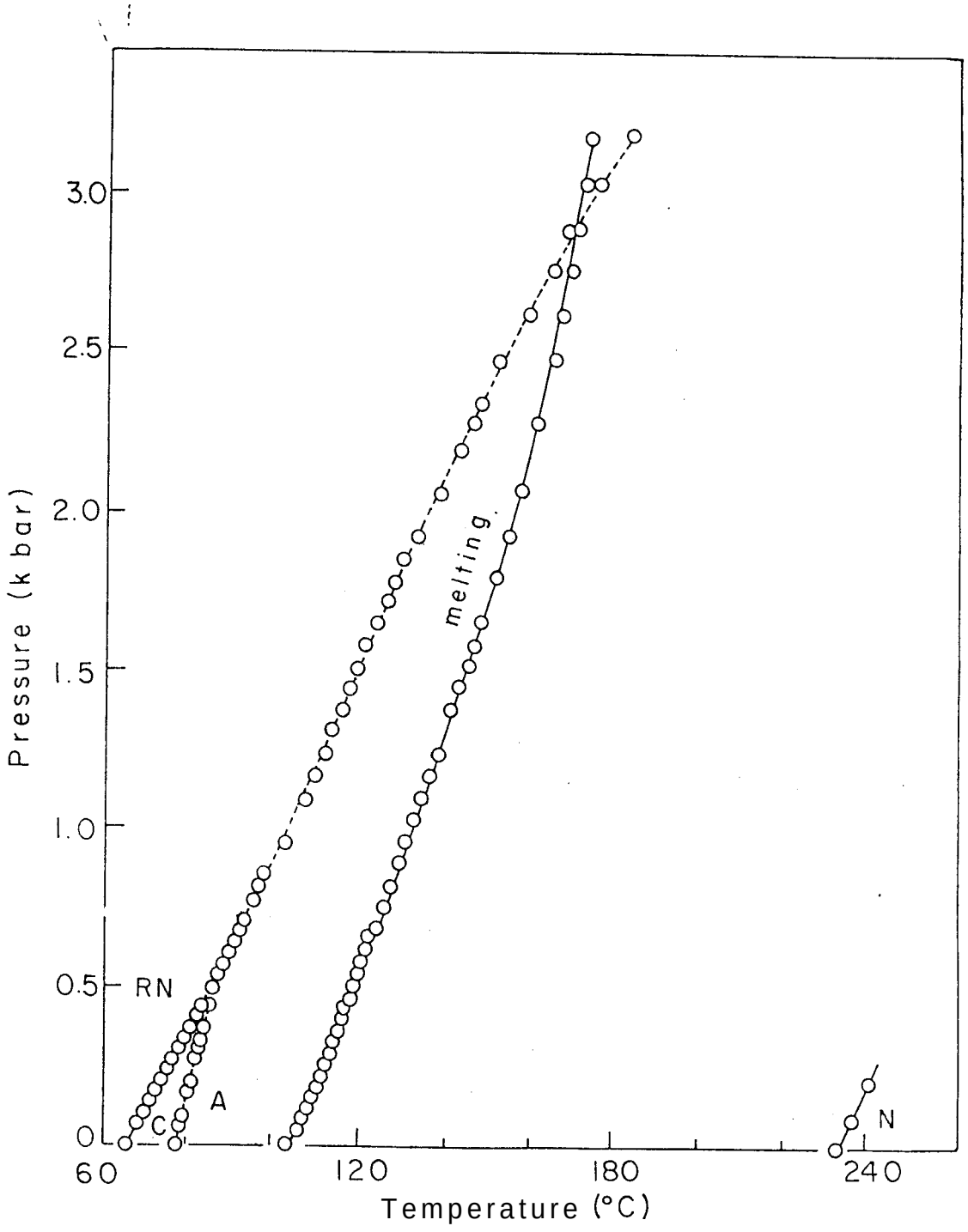

Figure 3.11 P-T diagram of DOBBCA obtained by Shashidhar et al[17]

the singularities are conspicuously absent. We shall now present the results of our precise experiments conducted to see if this is indeed true.

Figure 3.12 gives the results of our (more precise) studies obtained in the pressure range 0-800 bar. The RN-C-A point occurs at 0.55 ± 0.01 kbar and 86.8 ± 0.1°C. We also conducted high pressure DTA experiments (for details of the experimental techniques see Ref.20) to determine the nature of the transitions close to the RN-C-A point. A very high gain had to be used and it was observed that both the RN-C and C-A transitions which are second order at atmospheric pressure, remain so right up to the RN-C-A point. The RN-A transition, which exists only beyond 0.55 kbar was also found to be second order-like with somewhat larger pretransitional effects.

We shall now consider the topology of the P-T diagram in the immediate vicinity of the RN-C-A point as seen in the enlarged version of the diagram (fig.3.13). It may be mentioned here that the transitions become sharper as the RN-C-A point is approached and, as a consequence, the accuracy of the data close to the RN-C-A point is in fact better than that stated earlier. The following interesting features are seen from the diagram (fig.3.13).

1) The RN-C and RN-A boundaries are collinear at the RN-C-A point. No sinqularities are observed.

2) The C-A boundary which is initially straight, exhibits a curvature as it approaches the RN-C-A point.

It may be recalled here that around the same time as our experiments, Sigaud et al[21] reported the observation of a similar RN-C-A point - they refer-

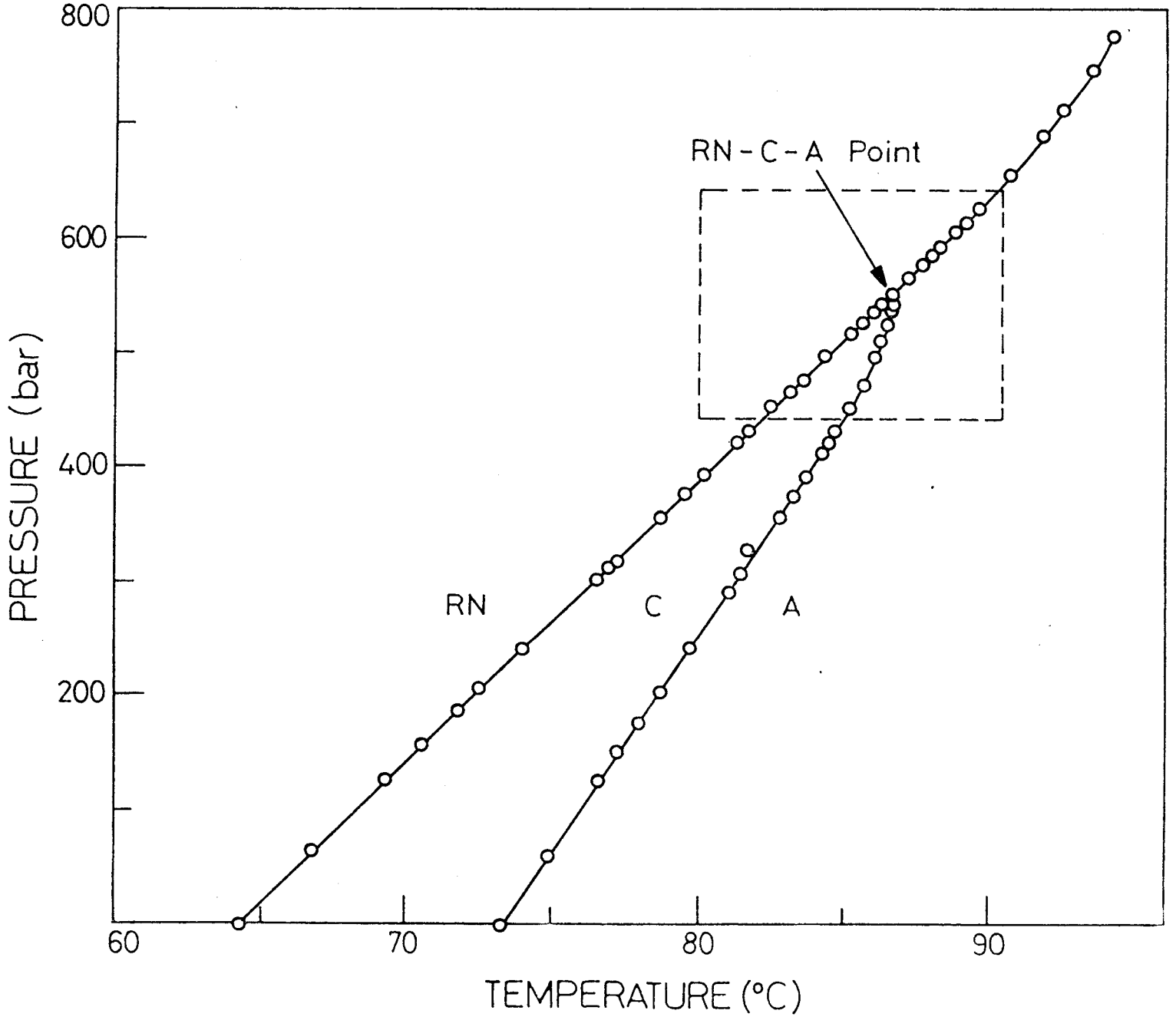

Figure 3.12 P-T diagram of DOBBCA showing the data for the RN, C and A phases upto 800 bar. The section enclosed in dashed lines is shown in an enlarged scale in fig. 3.13

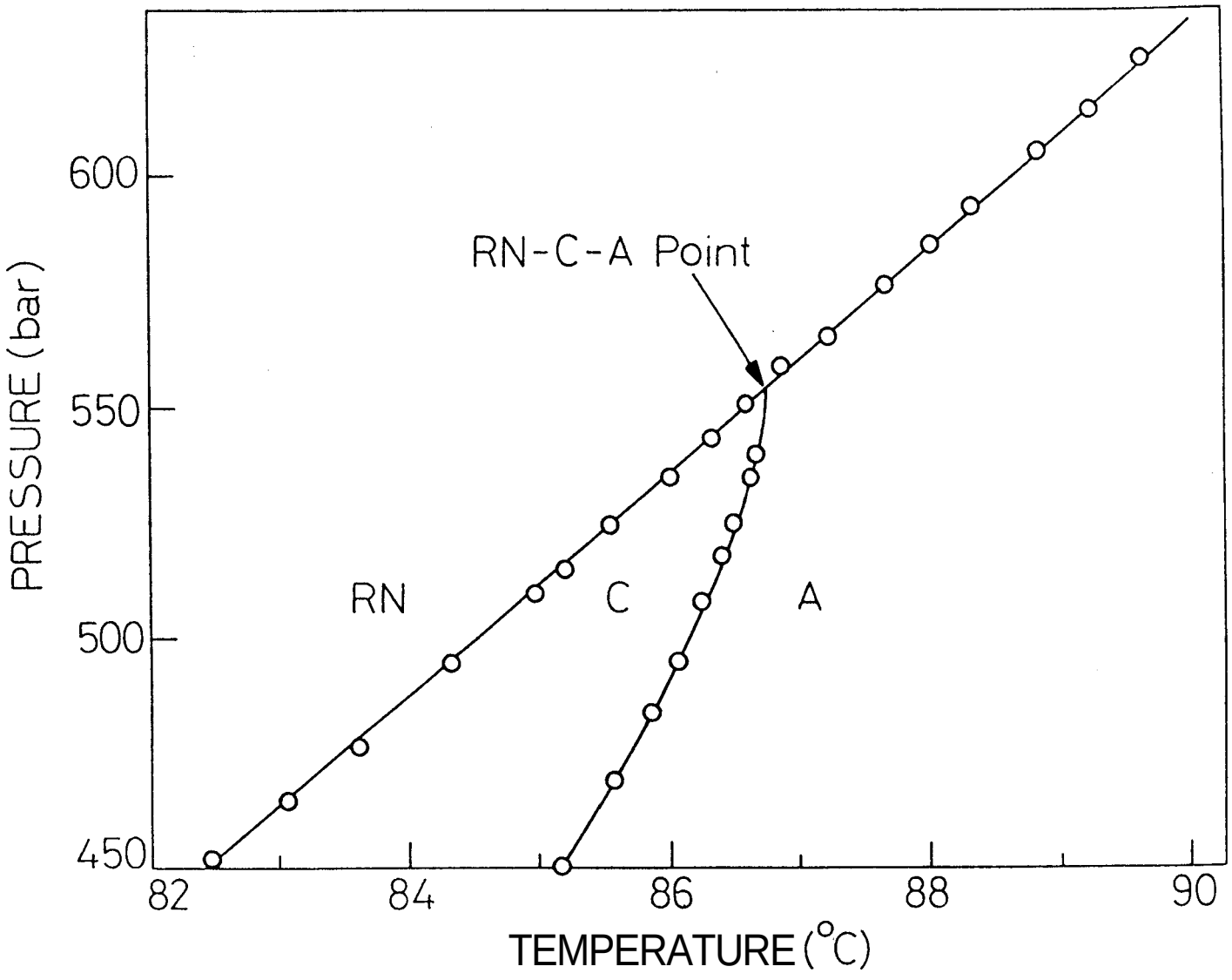

Figure 3.13 Enlarged section of the P-T diagram of DOBBCA in the vicinity of the RN-C-A multicritical point. No singularities are seen on the RN-C or RN-A lines

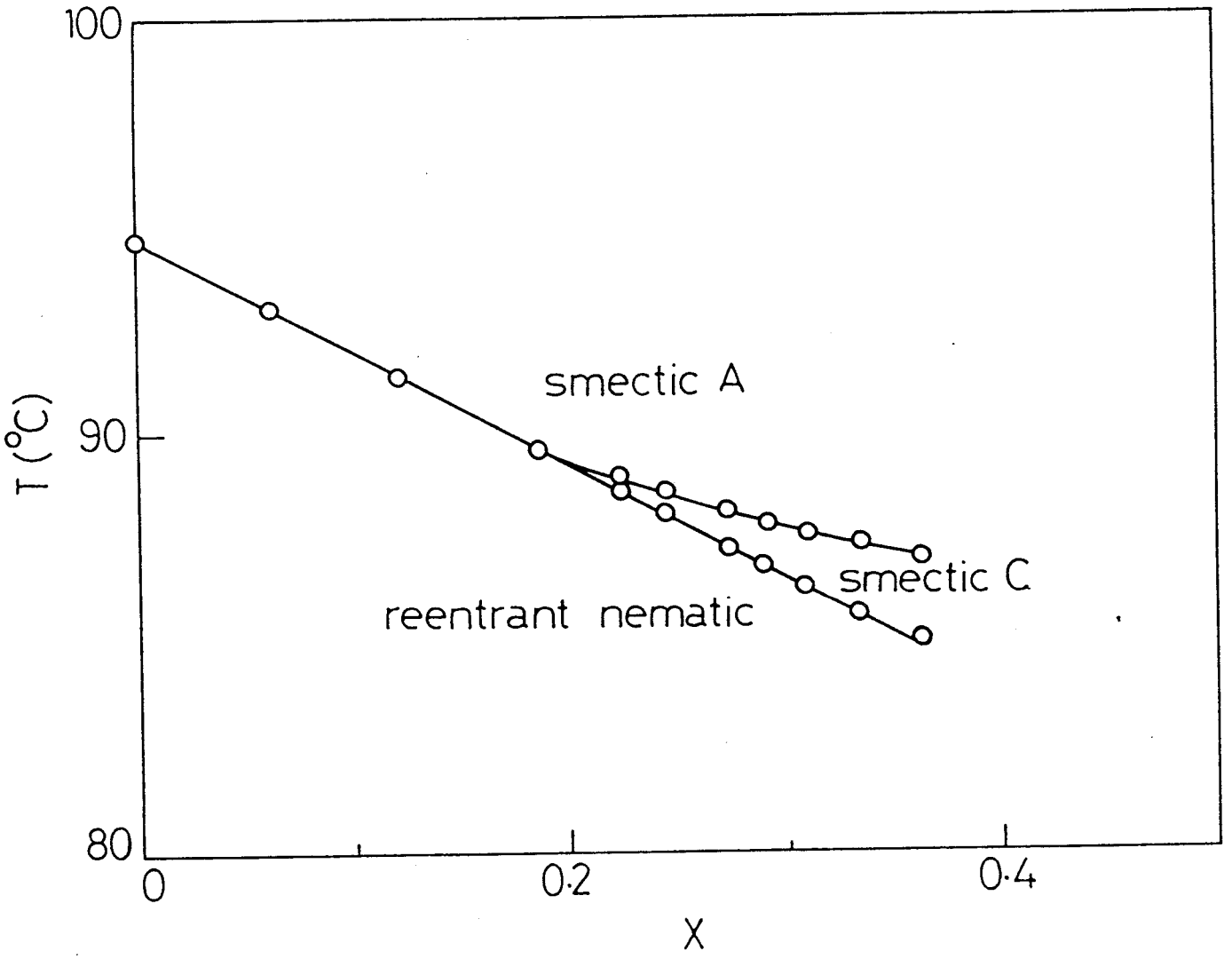

gure 3.14 Binary isobaric phase diagram of DOBBCA and 4-cyanobenzylidene-4'-(4"-decyloxybenzoyloxy)aniline. X denotes the mole fraction of DOBBCA in the mixture (from ref. 21)

red to it as the 'inverted NAC point' - in the T-X plane. Interestingly, the binary system studied by them consisted of DOBBCA as one of the constituents while the other compound was 4-cyanobenzylidene-4'-(4"-decyloxybenzoyloxy)aniline. These two compounds are identical in their molecular structure except that in the latter compound the direction of the linking Schiff base (-CH=N-) group is reversed. Fig.3.14 shows the T-X diagram obtained by Sigaud et al.[21] From a qualitative comparison between the P-T and T-X diagrams it is clear that the topology of the phase diagrams (close to the RN-C-A point) looks similar. We will compare this topology with that of the phase diagrams showing the NAC point at a later stage.

3.4.2 Studies on the NAC multicritical point

In this section we present the results of our high pressure studies on 7APCBB. The complete P-T diagram of 7APCBB showing the preliminary data for the NA, AC and NC transitions in the pressure range 1-600 bar is given in fig.3.15. It is seen that all the three lines are straight, away from the NAC point. But as they approach the multicritical point they curl up dramatically showing pronounced singularities.

The high resolution data (whose precision has already been discussed in Section 3.3) in the vicinity of the NAC point are shown in fig.3.16 on an enlarged scale. These data have been obtained from six independent sets of measurements, a fresh sample being loaded in the pressure cell each time. After every set of measurement the sample was taken out of the cell and

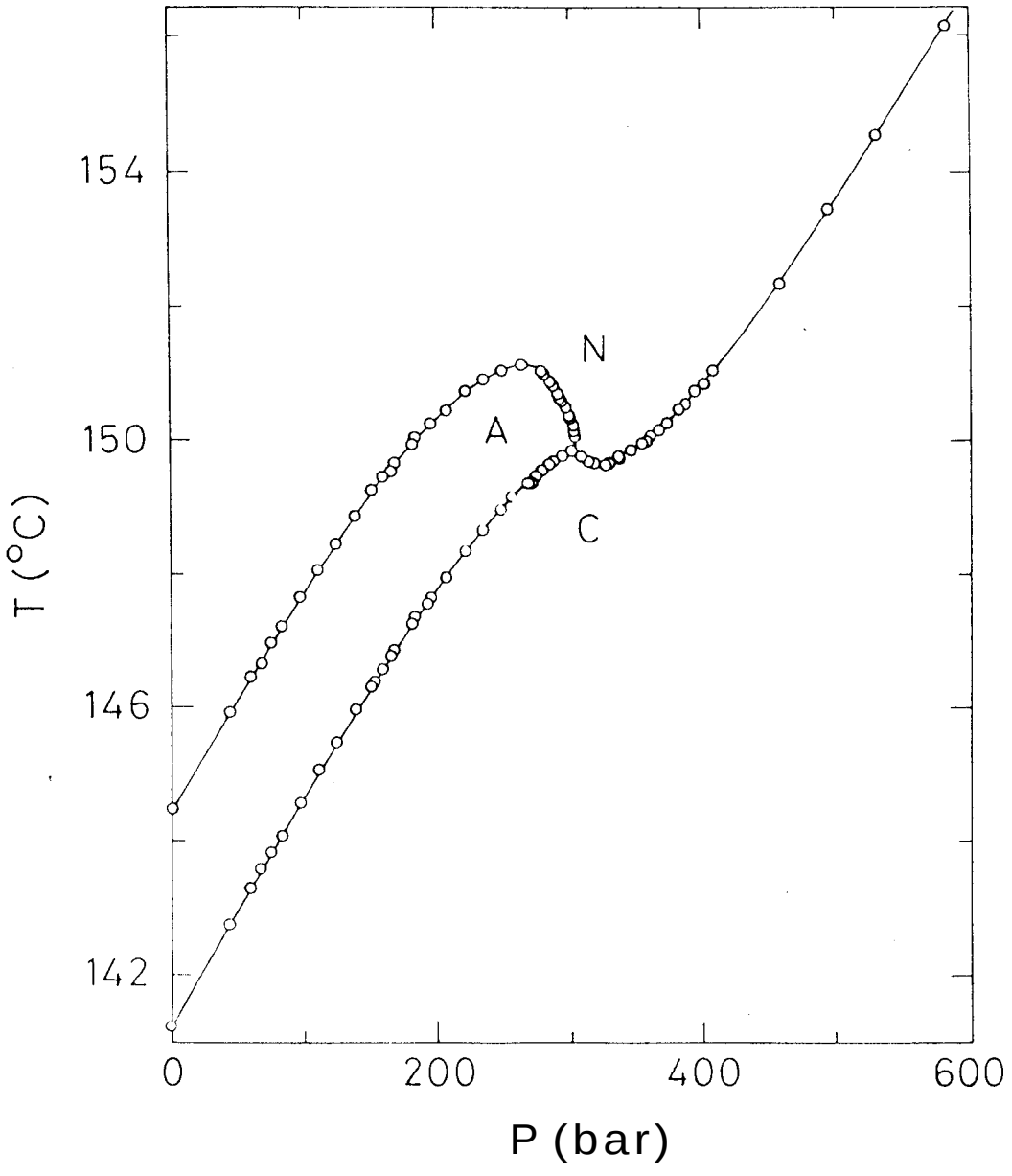

Figure 3.15 Pressure-temperature (P-T) diagram of 7APCBB showing NA, AC and NC transitions upto 600 bar. The solid lines are guides to the eye

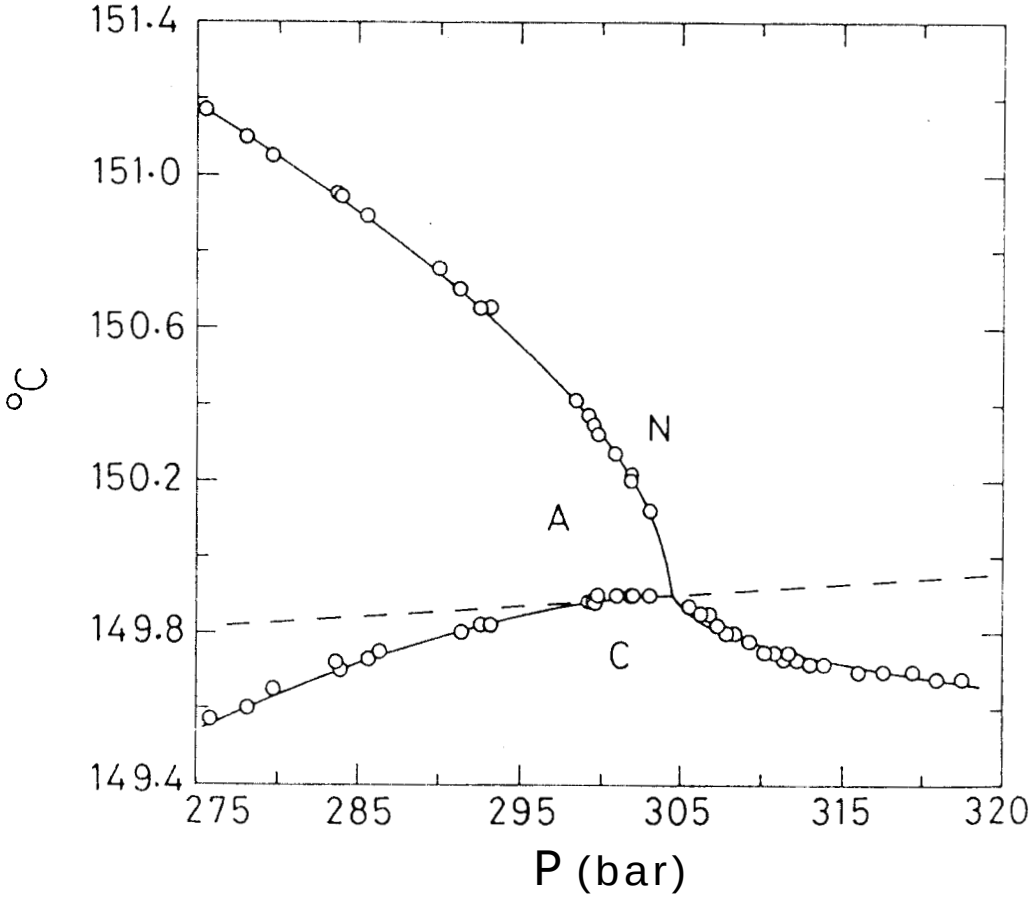

Figure 3.16 High resolution P-T diagram in the vicinity of the NAC multicritical point in 7APCBB. The solid lines are computer fits of our data (see Table 3.4) with equations 3a-3c representing the NA, NC and AC phase boundaries respectively. The dashed line represents the line corresponding to the best-fit B term

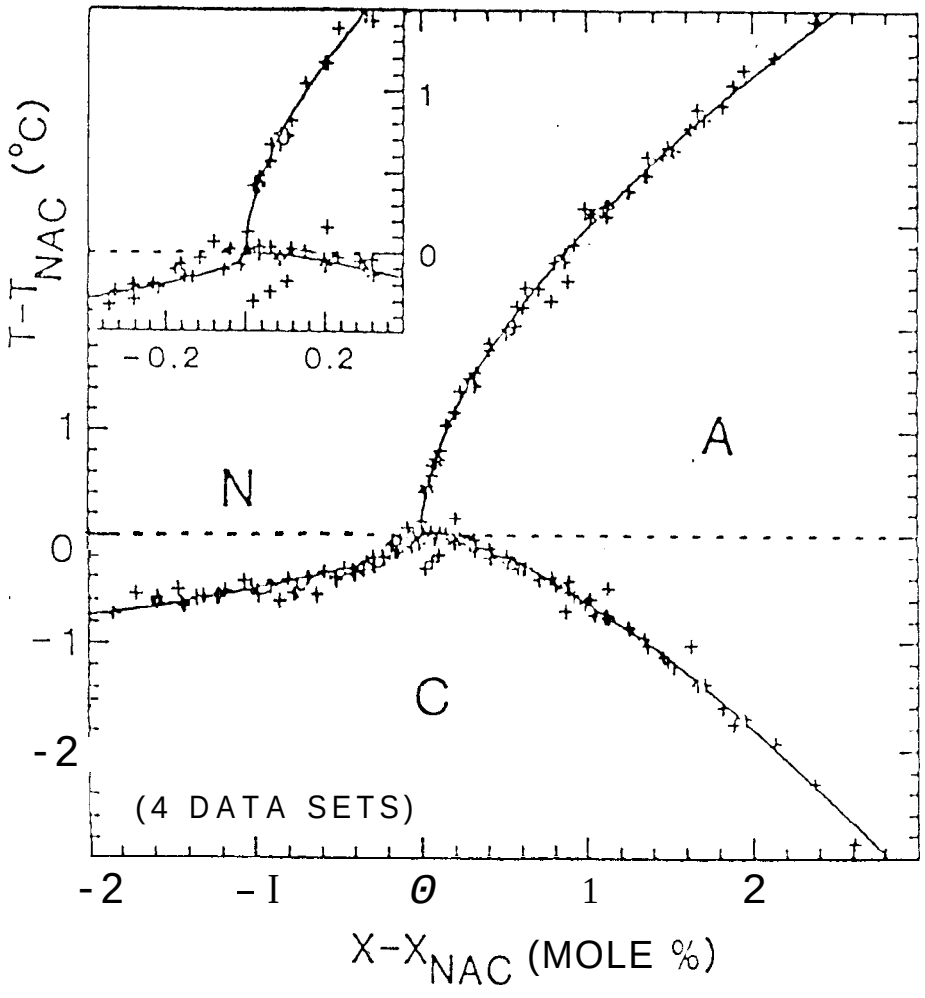

Figure 3.17 The universal temperature-concentration plot of Johnson (ref.22) showing the data for four binary liquid crystal systems shown separately in fig. 3.6

its A-N transition temperature at atmospheric pressure determined. If this did not agree exactly with the A-N transition temperature of the fresh sample, the data were rejected. Thus the possible influence of chemical degradation of the sample is precluded. It is clear by looking at the diagram (fig.3.16) that strong singularities are present in the vicinity of the multicritical point for all the three lines. This high resolution pressure-temperature diagram resembles closely the universal plot of Johnson,[22] shown in fig.3.17 wherein data for all the four binary systems mentioned earlier (Brisbin et al[14]) have been plotted together after suitable normalization. The striking similarity between the figs.3.16 and 3.17 is evident.

We shall now examine quantitatively the phase boundaries in the proximity of the NAC point. We have fitted our data for the NA, NC and AC phase boundaries individually to the following expressions which are similar to those of Brisbin et al[14]:

$$T_{NA} - T_{NAC} = A_{NA}(P_{NAC} - P_{NA})^{\eta_{NA}} + B(P_{NAC} - P_{NA}) \qquad [3\ a]$$

$$T_{NC} - T_{NAC} = A_{NC}(P_{NC} - P_{NAC})^{\eta_{NC}} + B(P_{NC} - P_{NAC}) \qquad [3\ b]$$

$$T_{AC} - T_{NAC} = A_{AC}(P_{NAC} - P_{AC})^{\eta_{AC}} + B(P_{NAC} - P_{AC}) \qquad [3\ c]$$

Following Brisbin et al,[14] we have carried out the computations, with the universality constraint $\eta_{NA} = \eta_{NC}$, η itself being a free parameter. The results of our computations carried out with the use of high resolution

data represented in fig. 3.16 are given in Table 3.4. Interestingly our values of η are, within statistical uncertainties, the same as those evaluated by Brisbin et al (see Table I , although the amplitude ratio A_{NA}/A_{NC} comes out to be - 3.02 ± 0.20 in our case, as compared to -5.96 ±1.3 of Brisbin et al. The remarkable fact that the η values obtained by us from the P-T diagram of single component system agree so closely with those evaluated from the T-X diagrams of four binary mixtures is, in our opinion, strong evidence to support the idea that NAC point exhibits universal behaviour. A noteworthy feature is that the scaling axes are the same as the experimental axes (P and T in our case, T and X in the case of Brisbin et al), rather than a linear combination of these variables. The simplicity of these results may perhaps be associated with the absence of coupling to density and concentration fluctuations.

As discussed earlier the topology of the phase diagrams showing the RN-C-A point was different from the universal topology of the NAC diagrams, the singularities being conspicuously absent near the RN-C-A point. The RN-C transition had a zero or immeasurably small latent heat at atmospheric pressure as well as at high pressures right up to the RN-C-A point. This could be due to the RN-C transition being far away in the temperature scale (about 180°C) from the nematic-isotropic transition. This would make the Brazovskii fluctuations[6] (which are believed to drive the NC transition first order[7]) to be extremely weak near the RN-C-A point which would explain the absence of any measurable latent heat at the RN-C transition. It would have the further effect that the bare correlation length would be very large. This in turn implies that the critical region may be too small to be experimentally approachable and could therefore account for the absence of pronounced singularities near the RN-C-A point.

TABLE 3.4

Best-fit parameters and values of χ^2 for individual fits of high-resolution data for the NA, NC and AC phase boundaries (of 7APCBB) with Eqs. (3a)-(3c) respectively. (See text for a detailed discussion)

B	0.003±0.001
T_{NAC}	149.9±0.02°C
P_{NAC}	304.5±0.1 bar
$\eta_{NA} = \eta_{NC}$	0.575±0.02
η_{AC}	1.523±0.02
A_{NA}	0.1 731±0.002
A_{NC}	-0.0574±0.003
A_{AC}	-0.0025±0.0004
χ^2_{NA}	1.056
χ^2_{NC}	0.969
χ^2_{AC}	0.911

3.4.3 Resume of the Current Theoretical and Experimental Understanding of the NAC Point

In the light of experimental results - both ours as well as those mentioned in the introductory section - let us compare the theoretical predictions and the experimental observations.

One of the two earliest models, viz., the Chu and McMillan[2] model was based on McMillan's microscopic theory[3] of the smectic C phase.

McMillan's theory centred around the electric dipole - dipole interaction, the dipolar orientational order bringing about the S_A-S_C transition. Thus the CM theory involved three order parameters, namely, the director **n** for the nematic order parameter, the complex order parameter $\psi(\mathbf{r})$ describing the smectic planes and another orientational order parameter $\beta(\mathbf{r})$ for the smectic C dipolar order. Neglecting the fluctuations in the order parameters, Chu and McMillan wrote the Landau free energy expression as

$$F = a\Psi_o^2 + \frac{1}{2} b\Psi_o^4 + e\beta_o^2\Psi_o^2 + \frac{1}{2} f\beta_o^4\Psi_o^2 \qquad [4]$$

where $\Psi = \Psi_o e^{(iq_z z + iq_x x)}$

$\boldsymbol{\beta} = \beta_o \mathbf{x}$

$\mathbf{n} = \mathbf{z}$

$a = a_o(T-T_1)$

$e = e_o(T-T_2)$

b and f are assumed to be positive and temperature independent.

It may be noted fhat in equation [4] β_o does not occur by itself in any term but always in combination with Ψ_o. This implies that the possibility of the existence of a biaxial nematic (i.e., tilt in the absence of layers, $\beta_o \neq 0$ $\Psi = 0$) is ruled out. Minimising F with respect to Ψ_o and β_o, the authors obtained a phase diagram where the continuous NA, NC and AC phase boundaries meet at a point $T_{NAC} = T_1 = T_2$. In addition to predicting the possibility of a NAC point, they also computed the Xray structure factor in the nematic phase close to the nematic - smectic C phase transition. The theory also found that all the three Frank elastic constants K_1, K_2 and K_3 diverge as the parallel coherence length ξ_{II}. This is in contrast to de Gennes theory[23] (which was based on Wilson's model[24]) where the elastic constants diverge as $\xi_{II}^{3/2}$. Apart from these, the Xray line profile was expected to be Lorentzian throughout the nematic phase. Also, the mass density fluctuations were expected to vary smoothly across the NAC phase diagram.

In the alternative approach by Chen and Lubensky[5] the smectic C phase is induced by the tilt of the nematic director relative to the layer normal. The tilt which is an additional parameter (not an order parameter) occurs when the coefficient of the transverse gradient term becomes negative. In the ordered phase the minimised free energy has the form

$$F = am^2 + um^4 + C_\perp k_\perp^2 m^2 + D_\perp k_\perp^4 m^4 \qquad [5]$$

where $m(\mathbf{r}) = \left[\int_D \frac{d^3k}{(2\pi)^3} e^{i\mathbf{k}.\mathbf{r}} \rho(\mathbf{k})\right]$ is the scalar order parameter; $\rho(\mathbf{k})$ being the

fourier transform of the centre of mass density $\rho(\mathbf{r})$. $\rho(\mathbf{r})$ is periodic with the fundamental wave vectors given by q_A and q_C in the smectic A and smectic C phases respectively. In the $(C_\perp, T)$ space, equation [5] leads to a phase diagram with an NAC point (fig. 3.2) at $(C_\perp = 0, T = T_{NAC}$. All the phase transitions, are continuous; however, the authors point out that owing to Brazovskii fluctuations[6] the NC transition may be driven first order.[7] The model predicts that the Xray scattering intensity in the nematic phase near the NAC point falls off in the transverse direction as $k_\perp^{-4}$. Also, the model predicts that at the NA transition K_2 and K_3 diverge but K_1 does not. This is in agreement with the predictions of de Gennes.[23] At the NC transition, however, the CL model predicts a ξ^2 divergence for K_1, K_2 and K_3 which is in disagreement with the de Gennes model[23] which predicts a $\xi^{3/2}$ divergence. As stated above, at the NAC point, $C_\perp = 0$ and hence, according to the CL theory, the NAC point is a Lifshitz Point.[1] At this point the authors calculated that K_3 diverges as $\xi_{||}$ while K_1 and K_2 are only slightly divergent.

Let us begin with a comparison of the topology of the NAC phase diagram obtained experimentally and those predicted by the two models. In the first phase diagram[9] ($\bar{7}S5/\bar{8}S5$ system) to show a NAC point, the AC and NC lines (i.e., the C line) have a common slope at the NAC point while the NA line approaches it obliquely. De Hoff et al[11] pointed out that this is in disagreement with the predictions of both the theories wherein the NA and NC lines have a common tangent with the AC line coming in obliquely.

The recent high resolution T-X diagrams of Brisbin et al[14] and our own pressure results presented in this chapter show that near the NAC point, the phase boundaries exhibit singularities. A notable feature is that the NA and NC lines have universal singularities. The explanation given by Brisbin et al[14] for the non observation of such singularities in the $\bar{7}S5/\bar{8}S5$ system[9,12] (which thus is in inconsistent with the universality concept) is that in this system the amplitude of the NC line divergence (A_{NC}) is very small. They also remark that the lower data density and precision of the $\bar{7}S5/\bar{8}S5$ experiments may be the other reasons for obtaining a non universal topology.

Let us now turn to calorimetric and Xray experiments. Subsequent to the observation of NAC point in $\bar{7}S5/\bar{8}S5$ system[9], De Hoff et al[11,12] performed thermodynamic measurements in the vicinity of the multicritical point. Using high resolution ac calorimetry in conjunction with quantitative DSC measurements, they obtained the NC transition entropy close to the NAC point. The NC transition entropy is of particular importance because the CM model predicts a continuous transition where as the CL model has a finite entropy for the transition. In the experiments of De Hoff et al[12] the specific heat contribution (obtained from ac calorimeter measurements) was subtracted from the enthalpy value got by DSC experiments. The results thus obtained by them are shown in fig. 3.18. It is seen that the NC transition entropy approaches zero with a concentration dependence that is linear over the entire range from 100% $\bar{7}S5$ to within a few percent of X_{NAC}. Within the last percent or so the ΔS_{NC} line curves towards the temperature

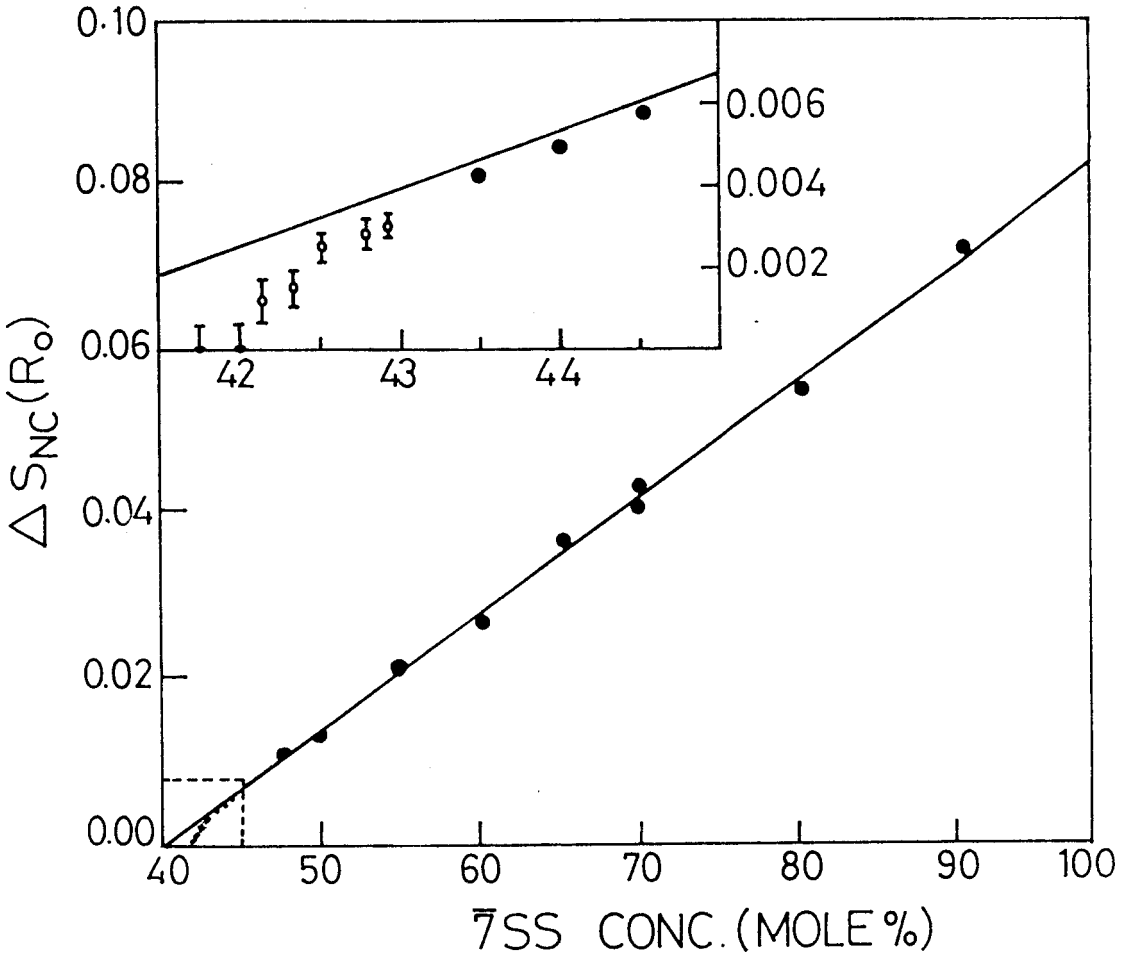

Figure 3.18 NC transition entropy versus concentration. Inset is an expansion of the region enclosed by dashed lines (from ref. 12)

axis and goes to zero. The NC transition entropy remaining finite throughout is in agreement with the CL model but in contradiction with the CM model. As no exactly solvable Lifshitz point model has been formulated for liquid crystalline systems, the authors compare the experimentally obtained critical exponent a for the thermal dependence of specific heat C_p, with that predicted for a magnetic Lifshitz point. The experimental value (α=0.67 ± 0.1) agreed very well with that of the theoretical one (a =0.6). Hence, but for the topology of the phase diagram, the results are in general agreement with the CL model.

To test the prediction of the CL model, viz., that near the NAC point the mass density fluctuations should have a $q_\perp^{-4}$ dependence rather than the conventional $q_\perp^{-2}$ behaviour and $\xi_\perp$ should approach zero as one approaches the NAC region, Safinya et al[13] took up high resolution Xray scattering studies on the $\bar{7}S5/\bar{8}S5$ system mentioned earlier. The Xray scattering cross section for the NA line can be written as

$$S(\mathbf{q}) = \frac{A\,\xi_{\parallel}^2}{1 + \xi_{\parallel}^2(q_{\parallel} - q_o)^2 + \xi_\perp^2\, q_\perp^2 + C_\perp\, \xi_\perp^4\, q_\perp^4} \qquad [\ 6\ ]$$

Safinya et al[13] carried out both longitudinal ($q_\parallel$ varied, $q_\perp$ = 0) as well as transverse ($q_\perp$ varied, $q_\parallel = q_o$) scans for each reduced temperature $t = (T-T_{NA})/T_{NA}$. Their scans obtained for $X_{\bar{7}S5}$ = 0.42 is shown in fig. 3.19. For this concentration both NA and AC were seen to be second order. The fits obtained by fitting the data to the expression [6] showed that both the transverse and the longitudinal scans are nearly identical Lorentzians. Fig. 3.20 shows the transverse correlation length $\xi_\perp$ obtained by them at a series of reduced

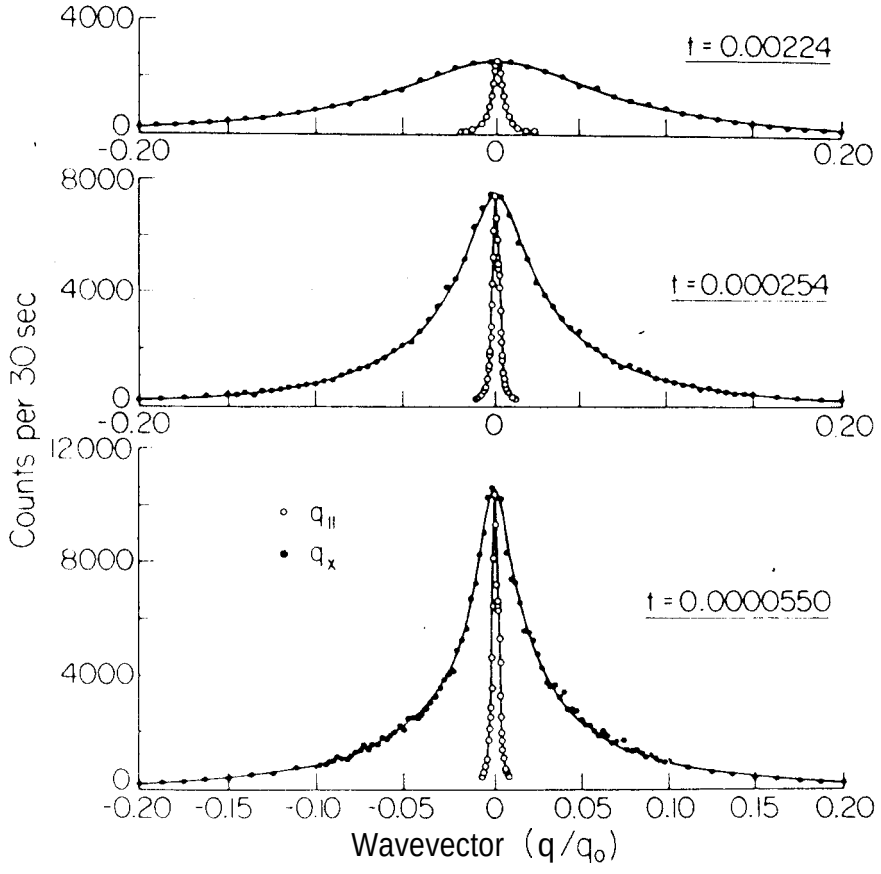

Figure 3.19 Transverse and longitudinal scans through the position $(0,0,q_o)$ for X = 0.42 (from ref. 13)

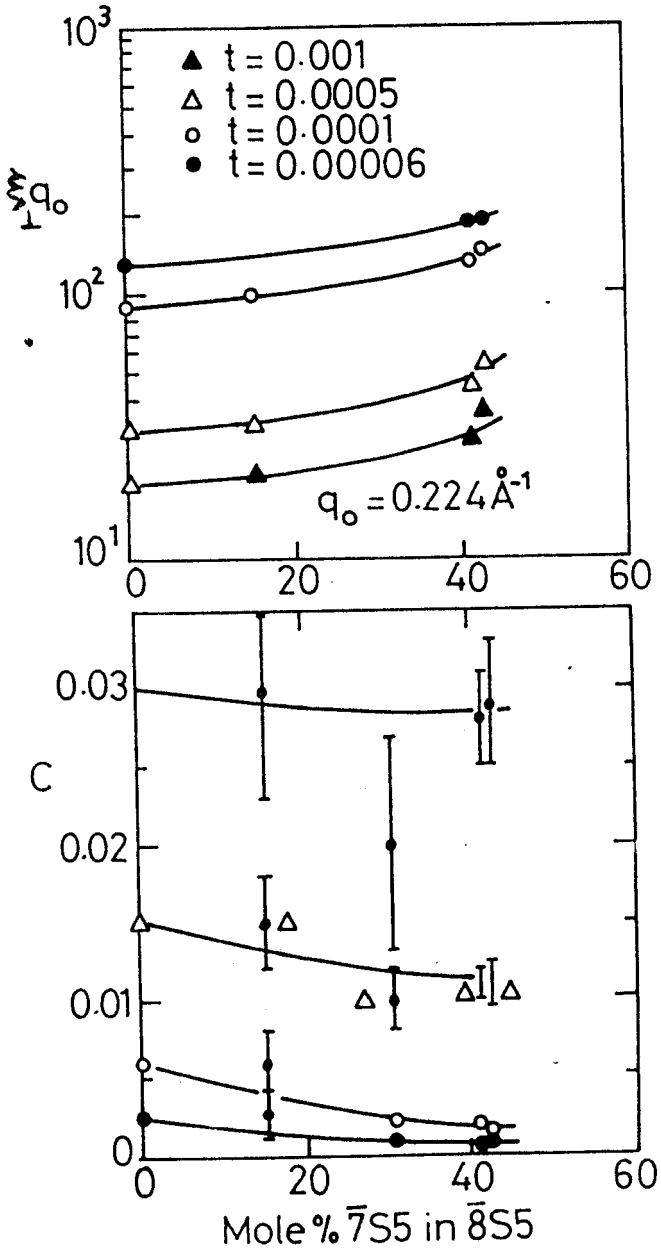

Figure 3.20 Upper figure: transverse correlation length $\xi_\perp q_o$ versus concentration of $\bar{7}$S5 at several reduced temperatures

Lower figure: coefficient of $\xi_\perp^4 q_\perp^4$ in equation–[6] at a series of reduced temperatures versus concentration of 7S5 (from ref. 13)

units. Also shown in the same figure is the evolution of the fourth order coefficient $C_\perp$. As it is seen both the quantities vary quite smoothly upto the NAC multicritical region with no evidence of the Chen and Lubensky prediction of $_L \longrightarrow 0$ at X_{NAC}; thus at variance with the Lifshitz point model for the NAC multicritical region. It may be recalled here that the CM model predicts that the mass density fluctuations should be Lorentzian throughout the nematic phase and that these fluctuations should vary smoothly across the NAC phase diagram. But another feature - tilt entering as an independent order parameter - was found to be incorrect and the CL approach of treating tilt as the transverse gradient of the density wave seemed to be consistent with the results.

Subsequently, Safinya et al[25] carried out a more elaborate high resolution Xray scattering study of the critical mass density fluctuations associated with the first order nematic - srnectic C transition in $\bar{7}S5/\bar{8}S5$ mixtures. These studies were carried out on five different concentrations, X = 0.70, 0.60, 0.50, 0.46 and 0.43; X_{NAC} being 0.422 (X is the mole fraction of $\bar{7}S5$ in the mixture). It was seen that the data obtained for $X \geq 0.46$ fits the expression [6] very well. When $C_\perp$ is positive this expression peaks for $q_\perp = 0$ and thus is characteristic of smectic A fluctuations. Therefore, the authors felt, in the nematic phase a crossover line $C_\perp(X,T) = 0$ separates regions with A - like ($C_\perp > 0$) from those with C - like ($C_\perp < 0$) critical behaviour (see fig. 3.21). It was also observed that along this line which terminates at X_{NAC}, $S(\mathbf{q})$ exhibits a $q_\perp^{-4}$-like behaviour - in accordance with the prediction of the CL model. An essential feature of the pretransitional smectic C scattering was

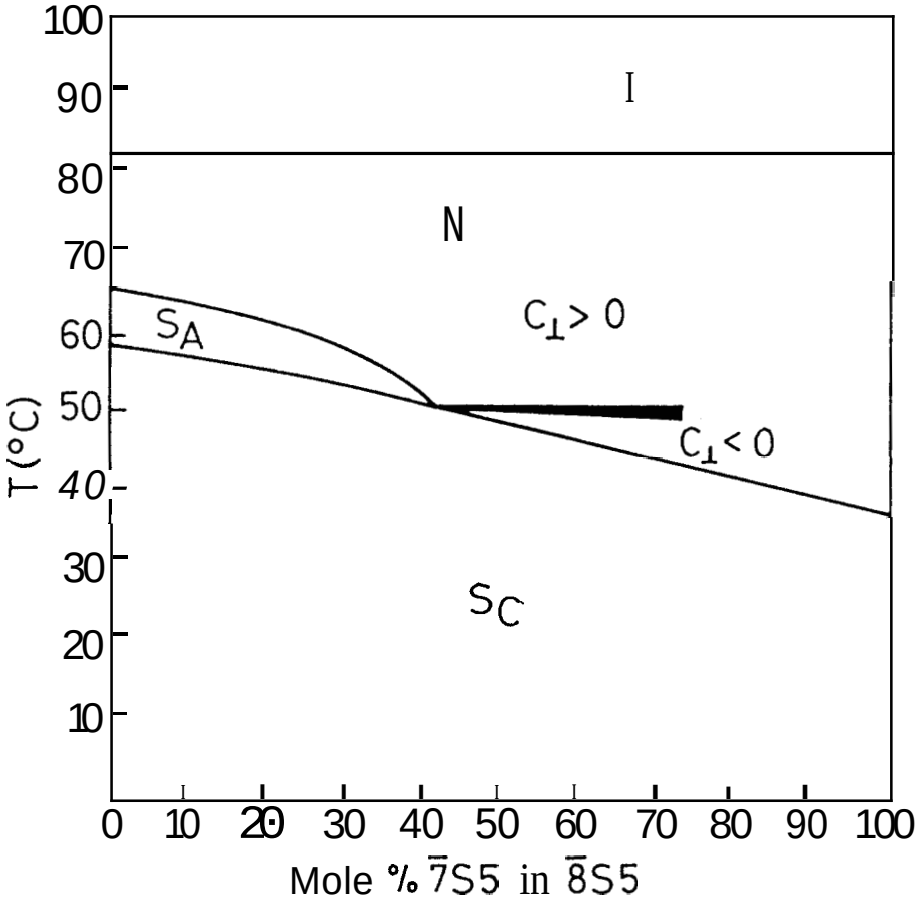

Figure 3.21 NAC phase diagram showing the crossover regime which separates regions of smectic A-like ($C > 0$) and smectic C-like ($C < 0$) critical fluctuations (from ref. 25)

the highly non Lorentzian transverse mass density fluctuations quantiatively accounted for by the CL model. The crossover region shown in fig. 3.21 appears to be hidden inside the first order NC line for the X ≃ 0.43 mixture. These results go well with the Lifshitz point model. But some important discrepancies like the proper location of the crossover line and nature of the fluctuations in the immediate neighbourhood of the NAC point, still remain.

The divergence of the Frank elastic constants can also help in understanding the nature of the NAC point. Witanachchi et al[26] have performed light scattering experiments on 7S5/8S5 mixtures in which they have followed the behaviour of the elastic constants. It is known that in the nematic phase the scattered intensity follows

$$I \alpha (K_i q^2 + K_3 q_z^2)^{-1} \qquad i = 1,2$$

where n is taken to lie along z and q is in the x-z plane ($\mathbf{q} = q_\perp \mathbf{x} + q_{II}\, z$). In actual experiments one can choose the scattering geometry such that $q_\perp$ is zero, so that the scattering intensity I is now proportional to $(K_3 q_z^2)^{-1}$. But when particularly the NA transition is involved the contribution to K_3 comes from both the intrinsic value K_{3o} plus a fluctuation part. Calculations on the basis of Schmid's analysis have shown that

$$K_3 = K_{3o} + K_o t^{-\zeta} \qquad [7]$$

The scattered intensity in terms of [7] will be

$$I = \frac{A}{K_{3o} + \delta K_o t^{-5}} \qquad [8]$$

It may be mentioned here that the CL model predicts a value of 1 for ζ where

as the C M model predicts $\zeta = 0.5$. In their light scattering experiments Witanachchi et al[26] found that the value of $(K_3 - K_{3_0})^{-1}$ varies linearly with temperature in accordance with equation [7] with $\zeta = 1$ over a wide range of temperature, in agreement with the predictions of Chen and Lubensky.[5] From their experiments in the smectic A, Smectic C and nematic phases for $X < X_{NAC}$ and smectic C and nematic phases for $X > X_{NAC}$, they concluded that the nature of the director fluctuations in the immediate vicinity of the NAC point is independent of whether X is greater or less than X_{NAC}.

Probably the best theoretical approach to the NAC problem is that due to Grinstein and Toner.[27] This theory based on the dislocation loop analysis uses the renomalization group technique. According to this approach, close to the NAC 'point, the NC transition (which is first order far from the NAC point), characterised by the simultaneous onset of long-range orientational (nematic-like) order and quasi long range positional order (C-like), occurs in two stages through a biaxial nematic N' phase. The NACN' multicritical point thus obtained by this theory is shown in fig. 3.22. As seen from the figure, at this point the NA and AC boundaries cross each other at a finite angle and pass through unaffected. In other words, through the NACN' point the AC and NN' boundaries form a single continuous curve as also the AN and CN' lines. The authors call this NACN' point which replaces the NAC point as a "decoupled tetracritical point". In this theory like in Toner's[28] analysis, the NA line is characterised by the "critical growth" of dislocational loops which are bounded in size at any point in the A phase. The AC line is characterised by critical fluctuations in the c director and the NACN' point

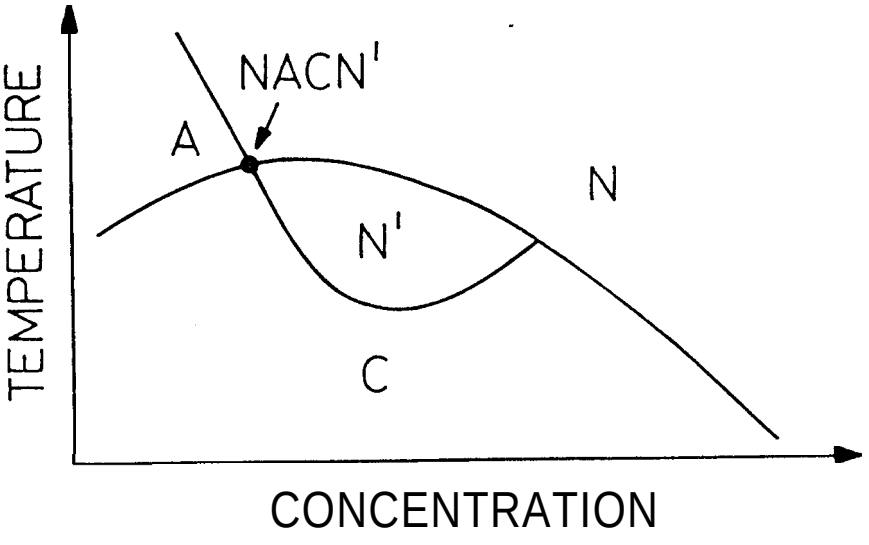

Figure 3.22 Phase diagram predicted by the dislocation-loop theory of Grinstein and Toner (ref. 27)

represents the simultaneous criticality of these two quantities. The decoupling mentioned above also implies that the AC and NN' transitions are identical. At these transitions the ordering is that of the ***c*** director. The dislocation loop-unbinding transitions AN and CN' are similarly identical. However, biaxial nematic phase which is predicted by the theory to exist near the multicritical point is yet to be observed experimentally either in binary mixtures or in single component systems.

Thus no theory of the NAC point is yet able to bring into agreement all the experimentally observed features. A complete understanding of this multicritical point still eludes us.

References

1. R.M.Hornreich, M.Luban and S.Shtrikmann, Phys. Rev. Lett., 35, 1678 (1975).

2. K.C.Chu and W.L.McMillan, Phys. Rev. A15, 1181 (1977).

3. W.L.McMillan, Phys. Rev., A8, 1921 (1973).

4. K.K.Kobayashi, Phys. Lett., 31A, 125 (1970); W.L.McMillan, Phys. Rev., A4, 1238 (1971); P.G.de Gennes, Solid State Commun., 10, 753 (1972).

5. J.H.Chen and T.C.Lubensky, Phys. Rev., A14, 1202 (1976).

6. S.A.Brazovskii, Sov. Phys. JETP, 41, 85 (1975).

7. J.Swift, Phys. Rev., A14, 2274 (1976).

8. D.Mukamel and R.M.Hornreich, J.Phys., C13, 161 (1980).

9. D.Johnson, D.Allender, R.De Hoff, C.Maze, E.Oppenheim and R.Reynolds, Phys. Rev., B16, 470 (1977).

10. G.Sigaud, F.Hardouin and M.F.Achard, Solid State Cornmun., 23, 35 (1977).

11. R.De Hoff, R.Biggers, D.Brisbin, R.Mahmood, C.Gooden and D.L.Johnson, Phys. Rev. Lett., 47, 664 (1981).

12. R.De Hoff, R.Biggers, D.Brisbin and D.L.Johnson, Phys. Rev., A25, 472 (1982).

13. C.R.Safinya, R.J.Birgeneau, J.D.Litster and M.E.Neubert, Phys. Rev. Lett., 47, 668 (1981).

14. D.Brisbin, D.L.Johnson, H.Fellner and M.E.Nubert, Phys. Rev. Lett., 50, 178 (1983).

15. R.Shashidhar, A.N.Kalkura and S.Chandrasekhar, Mol. Cryst. Liq. Cryst. Lett., 64, 101 (1980).

16. A.N.Kalkura, S.Krishna Prasad and R.Shashidhar, Mol. Cryst. Liq. Cryst., 99, 193 (1983).

17. R.Shashidhar, A.N.Kalkura and S.Chandrasekhar, Mol. Cryst. Liq. Cryst. Lett., 82, 311 (1982).

18. W.Weissflog, G.Pelzl, A.Wiegeleben and D.Demus, Mol. Cryst. Liq. Cryst. Lett., 56, 295 (1980).

19. For details of the high pressure cell see A.N.Kalkura, "High Pressure Optical Studies of Liquid Crystals", Ph.D. Thesis, University of Mysore (1982).

20. A.S.Reshamwala and R.Shashidhar, J.Phys., E10, 183 (1977).

21. G.Sigaud, Y.Guichard, F.Hardouin and L.G.Benguigui, Phys. Rev., A26, 3041 (1982).

22. D.L.Johnson (Private communication)

23. P.G.de Gennes, Mol. Cryst. Liq. Cryst., 21, 49 (1973).

24. K.G.Wilson and M.E.Fisher, Phys. Rev. Lett., 28, 240 (1972).

25. C.R.Safinya, L.J.Martinez-Miranda, M.Kaplan, J.D.Litster and R.J.Birgeneau, Phys. Rev. Lett., 50, 56 (1983).

26. S.Witanachchi, J.Huang and J.T.Ho, Phys. Rev. Lett., 50, 594 (1983).

27. G.Grinstein and J.Toner, Phys. Rev. Lett., 51, 2386 (1983).

28. J.Toner, Phys. Rev.,&, 462 (1982).